Available online at www.sciencedirect.com

ScienceDirect

Mendeleev Commun., 2022, **32**, 60–62

Mendeleev Communications

New coinage metal-coordinated intermetalloid E_{10} clusters $(R_3P)AuGe_9(Hyp)_3Pt(PPh_3)$ (R = Bu, Et)

Christian Gienger, Claudio Schrenk and Andreas Schnepf*

Chemistry Department, University of Tübingen, D-72076 Tübingen, Germany. Fax: +49 7071 28 2436; e-mail: andreas.schnepf@uni-tuebingen.de

DOI: 10.1016/j.mencom.2022.01.019

We present the synthesis and characterization of the intermetalloid clusters $R_3PAuGe_9(Hyp)_3Pt(PPh_3)$ [R = Et, Bu; Hyp = $Si(SiMe_3)_3$] obtained by the reaction of $R_3PAuGe_9(Hyp)_3$ (R = Et, Bu) with $Pt(PPh_3)_4$. The realized cluster enlargement is also known for the neutral cluster $Ge_9(Et)(Hyp)_3$, leading, however, to a different arrangement of substituents and different dynamics in the solution.

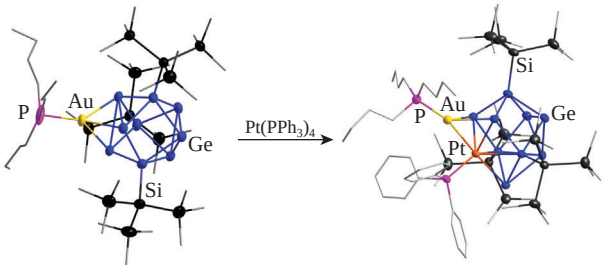

Keywords: intermetalloid clusters, germanium, metal insertion, cluster growth, NMR dynamics, X-ray diffraction.

The reactivity of group 14 metalloid clusters, especially $[Ge_9(Hyp)_3]^-$ [Hyp = $Si(SiMe_3)_3$], in connection with transition metal reagents, has become more and more attractive in recent years.[1] After the first synthesis of soluble $[Ge_9(Hyp)_3]^-$ by our group in 2003 *via* the disproportionation of a metastable Ge^IBr solution in the presence of LiHyp,[2] Li and Sevov found a more convenient synthesis route *via* readily available K_4Ge_9 in 2012.[3] After this route was established, many metalloid and intermetalloid clusters of $[Ge_9(Hyp)_3]^-$ with transition metals have been reported. In 2016, Sevov showed that the reaction of the neutral $EtGe_9(Hyp)_3$ cluster with $Pd(PPh_3)_4$ leads to a cluster enlargement to give an intermetalloid MGe_9 cluster.[4] This insertion is also possible with the remaining group 10 elements Ni and Pt, as shown by Fässler in 2018.[5] Thereby, it also became apparent that the cluster dynamics is frozen for the Pd and Pt derivatives. In 2018, we could show that not only cluster enlargement can take place since we successfully inserted Pt into the $(Hyp)_3Ge_9$–Zn–$Ge_9(Hyp)_3$ cluster to create the polynuclear chain compound HypZn–$Ge_9(Hyp)_3$–Pt–$Ge_9(Hyp)_3$–ZnHyp.[6] Additionally, Sevov showed that the reaction of $[Ge_9(EPr^i_3)_3]^-$ clusters (E = Sn, Si) gives intermetalloid $[Pd_3Ge_{18}(EPr^i_3)_6]^{2-}$ clusters.[7,8] Consequently, the fruitful reactivity between metalloid $[Ge_9R_3]^-$ clusters and group 10 reagents leads to very different outcomes if the kind or number of substituents at the metalloid germanium cluster is altered. We have recently synthesized the neutral intermetalloid clusters $(R_3P)AuGe_9(Hyp)_3$ (R = Et, Pr, Pr^i, Bu, Bu^t and Cy)[9] in good yields, and in the following, we present the first results of these compounds in the reaction with group 10 reagents.

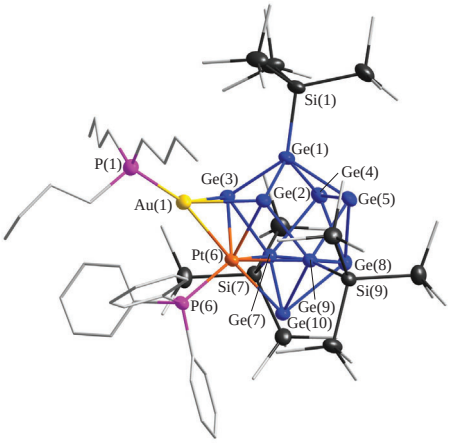

Figure 1 Molecular structure of $(Bu_3P)Au(PPh_3)PtGe_9(Hyp)_3$ **1** without hydrogen atoms. The organic groups are shown *via* a stick presentation and the other atoms as thermal ellipsoids (50% probability). Selected bond lengths (pm): Au(1)–P(1) 229.0(2), Pt(6)–P(6) 228.4(2), Au(1)–Pt(6) 268.28(6), Au(1)–Ge(2) 269.23(9), Au(1)–Ge(3) 280.91(9), Pt(6)–Ge(2) 261.80(9), Pt(6)–Ge(9) 274.72(9), Ge(1)–Ge(2) 251.13(12), Ge(1)–Ge(4) 255.79(12), Ge(2)–Ge(3) 303.45(13), Ge(4)–Ge(5) 270.88, Ge(5)–Ge(8) 262.31(12), Ge(8)–Ge(9) 267.53(12), Ge(1)–Si(1) 238.6(2). Selected angles (°): P(1)–Au(1)–Pt(6) 164.23(6), P(6)–Pt(6)–Au(1) 85.40(5), Si(1)–Ge(1)–Ge(4) 113.69(7), Pt(6)–Ge(10)–Ge(8) 98.51(3).

The reaction of $(Bu_3P)AuGe_9(Hyp)_3$ with $Pt(PPh_3)_4$ in THF leads to a color change of the solution from bright red to dark red and then to brown (for experimental details, see Online Supplementary Materials). After work-up of the reaction mixture, we obtained a product in the form of orange, rod-shaped crystals in 30% yield. X-ray crystal structure determination of these crystals revealed that the neutral intermetalloid cluster $(Bu_3P)Au(PPh_3)PtGe_9(Hyp)_3$ **1** was formed.† Within cluster **1**, the Pt atom is inserted into the cluster core, forming a *closo*-$PtGe_9$ cage, to which three Hyp substituents, Ph_3P and one $Au(Bu_3P)$ fragment are bound (Figure 1).

† *Crystal data for* **1**. $C_{57}H_{123}AuGe_9P_2PtSi_{12}$, M = 2252.93, monoclinic, space group $P2_1/c$, T = 150 K, a = 17.297(3), b = 22.874(4) and c = 26.885(4) Å, β = 100.198(4)°, Z = 4, V = 10469(3) Å^3, d_{calc} = 1.429 g cm^{-3}, $F(000)$ = 4332.0. Crystals of compound **1** were grown in *n*-heptane at –30 °C. An orange rod-shaped single crystal with dimensions 0.028 × 0.074 × 0.208 mm was selected, and 139808 reflections were measured. 18957 Independent reflections (R_{int} = 0.0739) were used for the structure solution and refinement. Final R factors: R_1 = 0.0473 [14435 reflections with $I > 2\sigma(I)$], wR_2 = 0.1168 (all reflections), GOOF = 1.111.

Crystal data for **2**. $C_{51}H_{111}AuGe_9P_2PtSi_{12}$, M = 2168.78, monoclinic, space group $P2_1/n$, T = 150 K, a = 15.6230(15), b = 26.637(3) and c = = 22.908(2) Å, β = 99.180(2)°, Z = 4, V = 9411.3(15) Å^3, d_{calc} = 1.531 g cm^{-3},

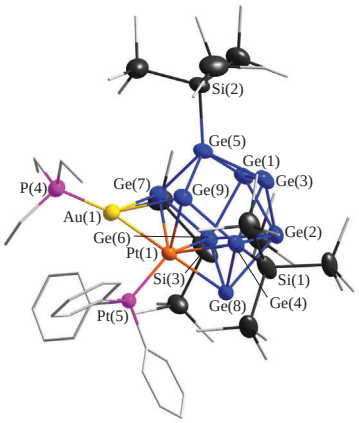

Figure 2 Molecular structure of $(Et_3P)Au(PPh_3)PtGe_9(Hyp)_3$ **2** without hydrogen atoms. The organic groups are shown *via* a stick presentation and the other atoms as thermal ellipsoids (50% probability). Selected bond lengths (pm): Au(1)–P(4) 229.2, Pt(1)–P(5) 226.9(3), Au(1)–Pt(1) 267.51(6), Au(1)–Ge(7) 281.57(12), Au(1)–Ge(9) 273.33(13), Pt(1)–Ge(7) 255.24(12), Pt(1)–Ge(6) 269.03(12), Ge(5)–Ge(1) 254.65(18), Ge(1)–Ge(3) 271.69(17), Ge(7)–Ge(9) 302.03(17), Ge(1)–Ge(2) 259.25(17), Ge(2)–Ge(8) 278.36(17), Ge(5)–Si(2) 238.8(3). Selected angles (°): Au(1)–Pt(1)–Ge(8) 177.73(4), P(5)–Pt(1)–Au(1) 82.79(7), Ge(8)–Ge(2)–Ge(3) 112.48(6).

On changing the starting compound to $(Et_3P)AuGe_9(Hyp)_3$, the isostructural intermetalloid cluster $(Et_3P)Au(PPh_3)PtGe_9(Hyp)_3$ **2** is isolated in 27% yield, and in the following, we will discuss only the structure of cluster **1** (molecular structure of cluster **2** is shown in Figure 2).

The metal core of $(Bu_3P)Au(PPh_3)PtGe_9(Hyp)_3$ **1** can be described as a distorted bicapped square antiprism built of nine germanium atoms and one platinum atom with the Au atom η^3-bonded to two Ge atoms and the Pt atom.† Three Hyp substituents are bound to the Ge_9Pt core *via* Ge–Si single bonds with an average length of 241.0 pm. Additionally, phosphine groups are bound to the gold and platinum atoms with Au–P and Pt–P distances of 229.0 and 228.4 pm, respectively. The *closo* structure of cluster **1** is in accordance with the Wade–Mingos rules[10] if we divide it into the $(Bu_3P)Au^+$ and $[(PPh_3)PtGe_9(Hyp)_3]^-$ fragments. In the latter, the germanium atoms with a Hyp substituent provide three electrons, and the bare germanium atoms contribute two electrons for cluster bonding, while the d^{10} Pt atom does not contribute any electrons for cluster bonding. With one additional electron from the negative charge, this results in a total of 22 electrons for cluster bonding ($2n + 2$ with $n = 10$). The Au–Ge distances of 269.2 and 280.9 pm in cluster **1** are longer than the corresponding distances in neutral $(Bu_3P)AuGe_9(Hyp)_3$, where Au–Ge distances of 260.9–262.0 pm are realized.[9] The bonding of the gold atom to the Ge_2 unit of the Ge_9Pt cage in cluster **1** gives a long Ge–Ge distance of 303.45 pm. Thus, the elongation is comparable to the elongation found in the neutral $(Bu_3P)AuGe_9(Hyp)_3$ cluster,[9] where the Ge–Ge distances amount to 296.2–301.0 pm, indicating comparable interactions. The Au–Pt distance of 268.3 pm in cluster **1** is longer than that found in the neutral compound $(PCy_3)Pt–Au–PPh_3$, where the Au–Pt distance is 254.1 pm.[11] The Au–Pt distance in cluster **1** is more comparable to the Au–Pt distances found in cluster compounds such as $[Pt_3(AuPPh_3)_5(\mu_2\text{-}CO)_2(PMe_3)_3]^+$ (264.8–300.7 pm).[12] Interestingly, the platinum atom is inserted into the $Ge_9(Hyp)_3$ core on the more shielded side, where the $AuPR_3$ group is bound as well, indicating that the Au–Pt interaction is important during the cluster enlargement. Additionally, if we compare clusters **1** and **2** with the previously mentioned $(Ph_3P)PtGe_9(Et)(Hyp)_3$, it is obvious that the substituents are bound to different germanium atoms. Hence, in the case of $(Ph_3P)PtGe_9(Et)(Hyp)_3$, both capping germanium atoms of the bicapped square antiprismatic arrangement bear a substituent (Hyp and Et). In the case of cluster **1**, only one capping germanium atom bears a Hyp substituent, while the other, to which the $Pt–PPh_3$ group is bound, is naked.

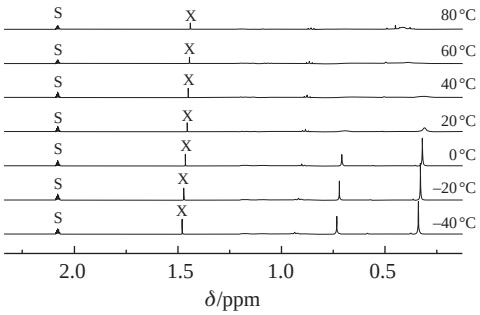

Figure 3 Variable-temperature proton NMR measurements of $(Bu_3P)Au(PPh_3)PtGe_9(Hyp)_3$ **1** in the temperature range from –40 to 80 °C in toluene-d_8 (S). The peak marked with X originates from cyclopentane, in which the sample was recrystallized.

It is apparent from the molecular structure of cluster **1** that two different hypersilyl groups are present in a 2 : 1 ratio, and indeed, in the proton NMR spectrum, we find two signals with an integral ratio of 2 : 1 for the protons of the hypersilyl groups. However, the signals are quite broad, indicating that there may be dynamics already present. Such dynamics in solution was also observed for the nickel derivative $Et(Hyp)_3Ge_9Ni(PPh_3)$.[5] In fact, variable-temperature NMR measurements show that the signals become much sharper on cooling, and we could also observe a coalescence on heating to 80 °C (Figure 3). Such dynamics was not observed in the Pt derivative $Et(Hyp)_3Ge_9Pt(PPh_3)$, showing that the substitution of the ethyl group for the $Au(PPh_3)$ group leads to a more dynamic compound, in which rapid migration of the Hyp substituents seems to be possible, as already discussed for the neutral compound $Et(Hyp)_3Ge_9$.[4,13]

Since the cluster site opposite to the $AuPR_3$ group is still open, further reactions might be possible. This possibility is further supported by the fact that according to quantum-chemical calculations, HOMO-1 is localized in this region (Figure S9, see Online Supplementary Materials).

In summary, we have presented the synthesis of the new intermetalloid *closo*-cluster compounds $(Bu_3P)Au(PPh_3)PtGe_9(Hyp)_3$ **1** and $(Et_3P)Au(PPh_3)PtGe_9(Hyp)_3$ **2**. Both compounds, obtained by the reaction of the neutral clusters $(R_3P)AuGe_9(Hyp)_3$ with $Pt(PPh_3)_4$, still have an open site for further build-up reactions.

F(000) = 4240.0. Crystals of compound **2** were grown in *n*-pentane at –30 °C. A single crystal fragment of a red block-shaped crystal with dimensions 0.057 × 0.079 × 0.202 mm was selected, and 142085 reflections were measured. 16108 Independent reflections (R_{int} = 0.1103) were used for the structure solution and refinement. Final *R* factors: R_1 = 0.0537 [10870 reflections with $I > 2\sigma(I)$], wR_2 = 0.1509 (all reflections), GOOF = 1.033.

X-ray diffraction data were collected on a Bruker APEX II DUO diffractometer equipped with an IμS microfocus sealed tube, QUAZAR optics for monochromated MoKα radiation (λ = 0.71073 Å) and an Oxford Cryosystems cryostat. Merging of equivalents and correction of absorption were carried out using the SADABS program. The structures were solved by direct methods and refined against F^2 for all observed reflections. Programs used: SHELXT and SHELXL[14] within the Olex2 program package.[15] Due to the disorder of co-crystallized solvent molecules (pentane, heptane), the SQUEEZE program[16] was used to identify in the case of $(Bu_3P)Au(PPh_3)PtGe_9(Hyp)_3$ **1** voids with a size of 2159 Å^3 containing 656 electrons. This amount corresponds to ten heptane molecules and two additional pentane molecules in a unit cell. In the case of $(Et_3P)Au(PPh_3)PtGe_9(Hyp)_3$ **2**, the volume of voids is 1176 Å^3, in which 286 electrons are located, which corresponds to six pentane molecules. The H atom positions were refined using a riding model.

CCDC 2102230 and 2102229 contain the supplementary crystallographic data for this paper. These data can be obtained free of charge from The Cambridge Crystallographic Data Centre *via* http://www.ccdc.cam.ac.uk.

In future investigations, we will also check the influence of the used neutral group 10 metal source and whether a different result will be obtained using, for example, $Pd(PPh_3)_4$ or $Ni(COD)_2$.

We thank the Deutsche Forschungsgemeinschaft (DFG) for financial support. The computational studies were supported by the bwHPC initiative and the bwHPC-C5 project provided through the associated compute services of the JUSTUS HPC facility at the University of Ulm. bwHPC and bwHPC-C5 (http://www.bwhpc-c5.de) are funded by the Ministry of Science, Research and the Arts Baden-Württemberg (MWK) and the Deutsche Forschungsgemeinschaft (DFG).

Online Supplementary Materials

Supplementary data associated with this article can be found in the online version at doi: 10.1016/j.mencom.2022.01.019.

References

1 O. Kysliak and A. Schnepf, in *Reference Module in Chemistry, Molecular Sciences and Chemical Engineering*, ed. J. Reedijk, Elsevier, Waltham, MA, 2017.
2 A. Schnepf, *Angew. Chem., Int. Ed.*, 2003, **42**, 2624.
3 F. Li and S. C. Sevov, *Inorg. Chem.*, 2012, **51**, 2706.
4 F. Li, A. Muñoz-Castro and S. C. Sevov, *Angew. Chem., Int. Ed.*, 2016, **55**, 8630.
5 S. Frischhut, F. Kaiser, W. Klein, M. Drees, F. E. Kühn and T. F. Fässler, *Organometallics*, 2018, **37**, 4560.
6 O. Kysliak, D. D. Nguyen, A. Z. Clayborne and A. Schnepf, *Inorg. Chem.*, 2018, **57**, 12603.
7 L. G. Perla and S. C. Sevov, *J. Am. Chem. Soc.*, 2016, **138**, 9795.
8 L. G. Perla, A. Muñoz-Castro and S. C. Sevov, *J. Am. Chem. Soc.*, 2017, **139**, 15176.
9 C. Gienger and A. Schnepf, *Z. Anorg. Allg. Chem.*, 2021, **647**, 1695.
10 K. Wade, *Adv. Inorg. Chem. Radiochem.*, 1976, **18**, 1.
11 J. Bauer, H. Braunschweig, A. Damme and K. Radacki, *Angew. Chem., Int. Ed.*, 2012, **51**, 10030.
12 N. de Silva, J. W. Laufenberg and L. F. Dahl, *Chem. Commun.*, 2006, 4437.
13 F. Li and S. C. Sevov, *J. Am. Chem. Soc.*, 2014, **136**, 12056.
14 (*a*) G. M. Sheldrick, *Acta Crystallogr., Sect. A: Found. Crystallogr.*, 2008, **64**, 112; (*b*) G. M. Sheldrick, *Acta Crystallogr., Sect. C: Struct. Chem.*, 2015, **71**, 3.
15 O. V. Dolomanov, L. J. Bourhis, R. J. Gildea, J. A. K. Howard and H. Puschmann, *J. Appl. Crystallogr.*, 2009, **42**, 339.
16 A. L. Spek, *Acta Crystallogr., Sect. D: Biol. Crystallogr.*, 2009, **65**, 148.

Received: 12th August 2021; Com. 21/6640